Received: 13 November 2022 | Revised: 13 May 2023 | Accepted: 31 May 2023

DOI: 10.1111/jne.13315

ORIGINAL ARTICLE

Journal of Neuroendocrinology WILEY

Impact of chemogenetic activation of dorsal vagal complex astrocytes in mice on adaptive glucoregulatory responses

Alastair J. MacDonald | Katherine R. Pye | Craig Beall | Kate L. J. Ellacott

Institute of Biomedical and Clinical Sciences, University of Exeter Medical School, Exeter, UK

Correspondence
Kate L. J. Ellacott Institute of Biomedical and Clinical Sciences, University of Exeter Medical School, RILD Building, Barrack Road, Exeter, EX2 5DW, UK.
Email: k.ellacott@exeter.ac.uk

Present address
Alastair J. MacDonald, Department of Physiology, University of California San Francisco, San Francisco, California, USA.

Funding information
Diabetes UK, Grant/Award Number: 19/0006035

Abstract

The dorsal vagal complex (DVC) regulates diverse aspects of physiology including food intake and blood glucose homeostasis. Astrocytes play an active role in regulating DVC function and, by extension, physiological parameters. DVC astrocytes in ex vivo slices respond to low tissue glucose. The response of neurons to low glucose is conditional on intact astrocyte signalling in slice preparations, suggesting astrocytes are primary sensors of glucose deprivation (glucoprivation). Based on these published findings we hypothesised that in vivo DVC astrocyte manipulation with chemogenetics would be sufficient to alter physiological responses that control blood glucose. We found that 2-h after systemic 2-DG-induced glucoprivation there were no observable changes in morphology of glial fibrillary acidic protein (GFAP)-immunoreactive DVC cells, specifically those in the nucleus of the solitary tract (NTS). Chemogenetic activation of DVC astrocytes was sufficient to suppress nocturnal food intake by reducing both meal size and meal number and this manipulation also suppressed 2-DG-induced glucoprivic food intake. Chemogenetic activation of DVC astrocytes did not increase basal blood glucose nor protect against insulin-induced hypoglycaemia. In male mice, chemogenetic DVC astrocyte activation did not alter glucose tolerance. In female mice, the initial glucose excursion was reduced in a glucose tolerance test, suggesting enhanced glucose absorption. Based on our data and published work, we propose that DVC astrocytes may play an indispensable homeostatic role, that is, are necessary to maintain the function of glucoregulatory neuronal circuitry, but alone their bulk activation is not sufficient to result in adaptive glucoregulatory responses. It is possible that there are state-dependent effects and/or DVC astrocyte subsets that have this specialised role, but this was unresolvable using the experimental approaches employed here.

KEYWORDS
astrocyte, brainstem, feeding, glucoprivic, hypoglycaemia

1 | INTRODUCTION

The dorsal vagal complex (DVC) is a brain centre involved in regulating many facets of homeostasis including food intake, digestion, cardiovascular reflexes, respiratory reflexes and glucose homeostasis.[1–5] Situated in the brainstem, the DVC consists of three nuclei: the area postrema (AP; a circumventricular organ), the nucleus of the solitary tract (NTS; a neuronal hub integrating input from the vagus nerves), and the

dorsal motor nucleus of the vagus (DMX; containing the cell bodies of preganglionic parasympathetic neurons that comprise the efferent branch of the vagus nerves). Of these constituent nuclei the NTS is the primary sensory integrator of signals from the periphery conveyed by the vagus nerves.

Neurons in the brainstem, particularly those in the NTS and ventrolateral medulla (VLM), are proposed to be intrinsic glucose sensors, sensing deviations in blood glucose (both hypo- and hyperglycaemia) and mediating physiological responses, including glucoprivic feeding and hormone secretion, to restore blood glucose.[5–8] Local tissue glucoprivation in the NTS and/or VLM induced by injection of 2-deoxyglucose (2-DG; an inhibitor of glycolysis) into the brain is sufficient to induce counter-regulatory food intake in rats, suggesting that cells in these sites can directly sense changes in glucose.[9] The potential importance of direct brainstem glucose sensing as part of counter-regulatory feeding responses is further supported by the observation that subdiaphragmatic vagotomy does not abolish glucoprivic stimulus-induced food intake in rats.[10]

Within the brainstem, catecholaminergic neurons, identified by their expression of tyrosine hydroxylase (TH) and/or dopamine beta-hydroxylase (DBH), are a key component of the circuitry underlying glucoprivic responses since their ablation eliminates glucoprivic feeding in rats[11] and their chemogenetic inhibition attenuates glucoprivic feeding in mice.[12] In addition, GABAergic NTS neurons have glucoregulatory capacity since their optogenetic or chemogenetic activation increases blood glucose and glucagon in mice, suggesting the ability of these neurons to drive homeostatic endocrine responses to hypoglycaemia.[13,14]

Although NTS^{TH} neurons are demonstrably required to generate glucoprivic feeding,[11,12] it is not clear whether they sense glucose levels cell-autonomously or instead are downstream of other glucose-sensing cells. Indeed, astrocytes in the NTS have been proposed as the primary cell type underlying low-glucose detection.[15] In support of this hypothesis, NTS astrocytes in ex vivo brain slices from both rats and mice show increases in intracellular calcium ($[Ca^{2+}]_i$) in response to low glucose conditions or bath application of 2-DG.[16–18] It appears that NTS astrocytes then relay this signal to neighbouring neurons (including NTS^{TH} neurons) by modulating extracellular purine levels.[17,18] NTS astrocyte activity and purinergic signalling is required for 2-DG-induced increases in blood glucose in anaesthetised rats, providing functional evidence for astrocyte detection of glucoprivation.[19] Glucose transporter 2 (GLUT2) is proposed to play a glucose-sensing role in astrocytes[20,21] as re-expression of GLUT2 in astrocytes of $GLUT2^{-/-}$ mice is sufficient to restore NTS sensitivity to glucoprivation.[20] In addition, the astrocyte Ca^{2+} response to bath application of low glucose in brain slices is abolished with pharmacological GLUT2 blockade.[21] Taken together, these data suggest NTS astrocytes can detect low glucose, modulate extracellular purine levels (possibly via direct release, i.e., gliotransmission) to excite neighbouring neurons, and drive physiological responses to restore blood glucose.[15]

Thus, evidence from ex vivo brain slice experiments suggest astrocytes in the NTS may be the primary sensors of local glucoprivation. While pharmacological inhibition of DVC astrocytes using fluorocitrate pretreatment prevented compensatory increases in blood glucose caused by systemic (subcutaneous) 2-DG administration,[19] the role of DVC astrocytes in detecting and orchestrating physiological responses to other deviations in blood glucose are less clear. Should DVC astrocytes be important in these processes, we reasoned that NTS astrocytes would show signs of morphological change following acute systemic glucoprivation induced by 2-DG. Second, we hypothesised that the chemogenetic activation of DVC astrocytes would be sufficient to modulate glucose homeostasis, for example by elevating blood glucose, amplifying glucoprivic feeding, and/or attenuating subsequent insulin-induced hypoglycaemia.

2 | MATERIALS AND METHODS

2.1 | Mice and housing

All animal studies were conducted in accordance with the UK Animals in Scientific Procedures Act 1986 (ASPA) and study plans were approved by the institutional Animal Welfare and Ethical Review Body at the University of Exeter.

C57BL/6J mice were either purchased from Charles River (Margate, UK) or bred in the University of Exeter Biological Services Unit for experiments. Homozygous Vglut2-IRES-Cre mice (016963, Jackson Laboratory) were bred in the University of Exeter Biological Services Unit from founder breeders purchased from the Jackson Laboratory. Male and female mice were used for experiments and data were pooled when a three-way ANOVA did not reveal a statistically significant effect of sex or a statistically significant interaction of sex and treatment (Table 1). Mice were aged >8 weeks by the time of experiment. Mice were housed in groups of 2–5 with ad libitum access to standard laboratory diet (EURodent diet [5LF2], LabDiet) and water in a 12:12 h light:dark cycle at 20 ± 2°C unless otherwise stated.

2.2 | Systemic acute 2-DG-induced glucoprivation

Mice were individually housed and handled by the experimenter for >6 days prior to the experiment. On the test day mice were injected with either saline or 2-DG (0.3 g/kg intraperitoneally [i.p.], Sigma) diluted in saline 2.5 h into the light phase, and food was removed from the cage. Two hours later mice were deeply anaesthetised with sodium pentobarbital and transcardially perfused with saline followed by 4% paraformaldehyde in 0.01 M phosphate buffered saline (PBS). Brains were dissected and post-fixed in 4% PFA in 0.01 M PBS for 24 h before being stored in 20% sucrose in 0.01 M PBS. Saline or 2-DG treatments were randomly assigned by coin toss, and the experimenter was blinded to the group allocations until image analysis was complete. The rostrocaudal "bins" used to quantify cell counts were as follows (all values—mm from Bregma): rostral 6.96–7.2, postremal 7.32–7.64, caudal 7.76–8. Sections were imaged at 10x magnification on an upright fluorescence microscope (Leica AF6000) and compared to a reference brain atlas[22] to determine the distance from Bregma. For colocalization analysis of FOS and GFAP-immunoreactivity, two postremal-level NTS sections were imaged at 20x magnification on a confocal microscope

TABLE 1 Results of three-way analysis of variance (ANOVA) of the effects, and interactions of sex, drug treatment and rostrocaudal (RC) position or time on FOS-immunoreactive (FOS-IR) cell number, GFAP-immunoreactive cell number, food intake, glucoprivic feeding, glucose tolerance test (GTT) or insulin tolerance test (ITT). Statistically significant effects ($p < .05$) are shown in bold font for clarity. For glucoprivic feeding only saline/2-deoxyglucose (2-DG) and clozapine-*N*-oxide (CNO)/2DG groups were analysed to examine the main effect of CNO.

Figure 1	RC position	2-DG	Sex	RC x 2-DG	RC X Sex	2-DG x Sex	RC x 2-DG x Sex
FOS-immunoreactive cell number	$\mathbf{F_{(2,12)} = 31.67, p < .0001}$	$\mathbf{F_{(1,6)} = 88.94, p < .0001}$	$F_{(1,6)} = 0.66, p = .45$	$\mathbf{F_{(2,12)} = 28.22, p < .0001}$	$F_{(2,12)} = 0.88, p = .44$	$F_{(1,6)} = 0.12, p = .74$	$F_{(2,12)} = 3.17, p = .08$
GFAP-immunoreactive cell number	$\mathbf{F_{(2,12)} = 44.58, p < .0001}$	$F_{(1,6)} = 0.83, p = .40$	$F_{(1,6)} = 1.83, p = .23$	$F_{(2,12)} = 2.87, p = .10$	$F_{(2,12)} = 1.37, p = .29$	$F_{(1,6)} = 0.27, p = .62$	$F_{(2,12)} = 1.75, p = .22$
Figures 2–4	**Time**	**CNO**	**Sex**	**Time x CNO**	**Time x Sex**	**CNO x Sex**	**Time x CNO x Sex**
Food intake	$\mathbf{F_{(23,253)} = 212.5, p < .0001}$	$\mathbf{F_{(1,11)} = 37.72, p < .0001}$	$\mathbf{F_{(1,11)} = 5.085, p = .045}$	$\mathbf{F_{(23,253)} = 18.72, p < .0001}$	$\mathbf{F_{(23,253)} = 2.7, p < .0001}$	$F_{(1,11)} = 0.16, p = .70$	$F_{(23,253)} = 0.23, p > .99$
Glucoprivic feeding	$\mathbf{F_{(4,48)} = 338.6, p < .0001}$	$\mathbf{F_{(1,12)} = 32.52, p < .0001}$	$F_{(1,12)} = 0.58, p = .46$	$\mathbf{F_{(4,48)} = 19.38, p < .0001}$	$F_{(4,48)} = 1.30, p = .28$	$F_{(1,12)} = 0.36, p = .56$	$F_{(4,48)} = 1.00, p = .42$
GTT	$\mathbf{F_{(6,72)} = 58.91, p < .0001}$	$F_{(1,12)} = 1.03, p = .33$	$\mathbf{F_{(1,12)} = 8.036, p = .015}$	$\mathbf{F_{(6,72)} = 5.81, p < .0001}$	$F_{(6,72)} = 1.01, p = .37$	$F_{(1,12)} = 2.35, p = .15$	$F_{(6,72)} = 0.39, p = .88$
ITT	$\mathbf{F_{(6,72)} = 61.95, p < .0001}$	$F_{(1,12)} = 0.18, p = .68$	$F_{(1,12)} = 4.277, p = .06$	$F_{(6,72)} = 1.18, p < 0.33$	$F_{(6,72)} = 1.24, p = .30$	$F_{(1,12)} = 0.06, p = .80$	$F_{(6,72)} = 0.46, p = .84$

Note: Bold indicates statistically significant value ($p < .05$).

(Leica DMi8) and mean cell counts from these sections were calculated for each mouse ($n = 8$ mice per group, 5 male, 3 female).

2.3 | Viral vector injection surgery

Viral vectors were delivered to the DVC as described previously.[23,24] In brief, mice were anaesthetised with ketamine (70 mg/kg) and medetomidine (0.5 mg/kg) administered as a cocktail i.p. The skin on the back of the head and neck was shaved and the mouse was placed in a stereotaxic frame. Under aseptic conditions, the skin was incised, and the muscles parted to expose the atlanto-occipital membrane. This membrane was then incised, and a Hamilton needle inserted into the left side of the brain (from obex r/c 0 mm, m/l 0.2 mm, d/v 0.5 mm) at a 25° angle. Then, 180 nL of viral vector was injected at a rate of 100 nL/min and the needle was kept in place for 2 min after the injection. This process was then repeated on the contralateral (right) side and the wound was closed with sutures in the muscle and skin. The mouse was subcutaneously injected with carprofen (5 mg/kg) and atipamezole (1 mg/kg) and transferred to a heated (24–26°C) recovery cage. The following morning mice received a second injection of carprofen (5 mg/kg). Mice were given >3 weeks to allow for recovery and viral expression before being used in experiments. Viral vectors used were AAV9/2-hGFAP-hM3Dq-mCherry (ETH Zurich Viral Vector Facility, Zurich, Switzerland; titre = 5×10^8 viral genomes/mL), AAV5/2-hGFAP-mCherry (ViGene Biosciences; titre = 3.89×10^{13}) or AAV5/2-hSyn-DIO-eGFP (ETH Zurich Viral Vector Facility) and were diluted 1:2 in sterile saline prior to injection when one vector was injected. When two vectors were coinjected they were mixed 1:1:1 with sterile saline.

2.4 | Food intake, water intake and activity monitoring

Mice were individually housed in Promethion metabolic monitoring cages (Sable Systems Europe) which contained three sensors: a mass monitor attached to the food hopper, a mass monitor attached to the water bottle, and an XY-beam array surrounding the cage. These permitted the accurate quantification of food intake, water intake and activity using the Promethion system for data acquisition and a macro for data analysis. On the day of the experiment mice were injected i.p. with saline or clozapine-*N*-oxide (CNO; 1 mg/kg, Tocris/Bio-Techne) immediately prior to lights off. Data were then acquired for 23 h. Drug order was not randomised due to the potential duration of CNO-mediated effects and for this reason the experimenter was not blinded. Saline was given first followed at least 72 h later by CNO. Following this, the same mice were used for glucose tolerance testing (see below).

2.5 | Glucoprivic feeding

The protocol for assessing glucoprivic feeding was modified from Lewis et al.[25] Mice were individually housed and habituated to

experimenter handling for >6 days prior to the experiment. First, mice were injected with saline (i.p.) 3.5 h into the light phase and received a second injection of saline 30 min later. Food intake was then measured manually 1, 2, 4, 8 and 24 h later. On the subsequent test days mice were injected with either saline or CNO (1 mg/kg) i.p. 3.5 h into the light phase followed by 2-DG (0.4 g/kg i.p.) 30 min later. Food intake was again manually measured at 1, 2, 4, 8 and 24 h. Test days were separated by at least 72 h. The allocation of saline or CNO was randomised by coin toss and the investigator was blinded to this allocation until the conclusion of the experiment. On the final day, all mice received CNO (1 mg/kg i.p.) 3.5 h into the light phase and saline 30 min later. Food intake was again measured at 1, 2, 4, 8 and 24 h following the second injection. Following this, the same mice were used for insulin tolerance testing (see below).

2.6 | Glucose and insulin tolerance tests

Individually housed mice were transferred to a clean cage with no food 2.5 h into the light phase. Then, 3.5 h later the mice were injected i.p. with either saline or CNO (1 mg/kg) and EMLA cream (Covetrus) was applied to the tip of the tail. Thirty minutes later (6 h into the light phase) the tip of the tail was cut with scissors and blood glucose measured with a handheld glucometer (Accu-chek, Roche). Mice were immediately injected with glucose (2 g/kg, Sigma) or insulin (1 U/kg, Actrapid, NovoNordisk) i.p. and returned to the cage. Blood glucose was measured from the same tail cut 15, 30, 45, 60, 90 and 120 min following injection. Then, 10–14 days later the test was repeated with the opposite drug (saline or CNO) given in the first injection. The initial drug allocation was randomised by coin toss and the investigator was blinded to this allocation until after the experiment concluded.

2.7 | Perfusion and histology

All viral-vector injected mice were perfused as described above ("Systemic acute 2-DG-induced glucoprivation") to confirm transduction and quantify viral spread. In some cases, mice were injected with CNO (1 mg/kg i.p.) 2 h prior to perfusion and food was removed from the cage at this time. Fixed brains were cut into 30 μm thick coronal sections containing the DVC on a freezing sledge microtome (Bright Instruments). For immunohistochemical staining these sections were blocked in 0.01 M PBS containing 5% normal donkey serum (Sigma) and 0.3% triton X-100 (Sigma) for 1 h at room temperature, then incubated with a primary antibody (Table 2) diluted in 1% normal donkey serum and 0.3% triton X-100 in PBS either for 1 h at room temperature or overnight at 4°C. Sections were then washed 8 x 5 min in PBS and incubated with a secondary antibody (Table 2) diluted 1:500 in 0.3% triton X-100 in PBS. Sections were then washed 8 x 5 min in PBS before being mounted onto glass slides and cover-slipped with fluoroshield mounting medium with DAPI (AbCam). Dual staining was performed with sequential primary-secondary incubations. Images were acquired on an upright microscope (Leica AF6000; injection mapping) or a confocal microscope (Leica DMi8; cell counting, colocalisation, morphological analysis) and analysed in FIJI[26] using simple neurite tracer (SNT) for morphological and Sholl analysis.[27]

To examine the efficiency and specificity of viral transduction, three postremal NTS sections were imaged from three mice (one section per mouse) at 40x magnification in a single *z*-plane. The number of GFAP (38.67 ± 5.36) and NeuN (67.33 ± 9.61) immunoreactive cells were counted in each image and then the percentage of those cells spatially associated with the diffuse mCherry immunoreactivity was calculated.

TABLE 2 Primary and secondary antibodies used.

Primary antibody	Manufacturer, catalogue number	Dilution
Mouse anti-GFAP	Millipore (MAB360)	1:5000
Rabbit anti-NeuN	AbCam (ab177487)	1:2000
Rabbit anti-FOS	Cell Signalling Technologies (2250 s)	1:1000
Goat anti-mCherry	Sicgen (CAB0040-200)	1:1000
Sheep anti-TH	Millipore (AB1542)	1:1000
Secondary antibody	**Manufacturer, catalogue number**	**Dilution**
Donkey anti-mouse Alexa Fluor 488	Invitrogen (A21202)	1:500
Donkey anti-mouse Alexa Fluor 568	Invitrogen, A10037	1:500
Donkey anti-rabbit Alexa Fluor 488	Invitrogen, A21206	1:500
Donkey anti-rabbit Alexa Fluor 647	Invitrogen, A31573	1:500
Donkey anti-goat Alexa Fluor 594	Invitrogen, A11058	1:500
Donkey anti-sheep Alexa Fluor 488	Invitrogen, A11015	1:500

Abbreviations: GFAP, glial-fibrillary acidic protein; NeuN, neuronal nuclear marker a.k.a Fox-3; TH, tyrosine hydroxylase.

2.8 | Statistical analysis

All values were collated in Prism 9 (GraphPad) for tests of statistical significance ($p < .05$). For between-subjects design with one value per subject, unpaired *t*-tests were used. For within-subjects design with two values per subject, paired *t*-tests were used. For between-subjects design with multiple values per subject, two-way ANOVA was used with Sidak's post hoc test applied to compare between column means. For within-subjects design with two values per subject over time, two-way repeated measure ANOVA was used with Sidak's post hoc test applied to compare between column means. For within-subjects design with three or more values per subject over time, two-way repeated measure ANOVA was used with Greenhouse–Geisser correction and Sidak's post hoc test applied to compare between column means. Three-way ANOVA was used to assess any statistically significant effects of sex or a statistically significant interactions between sex and treatment. No tests for normality or equal variance were performed and therefore all statistical tests assume a normal

distribution and equal variance. Samples in statistical tests were independent since only one data point per mouse was included and all mice were randomised to a condition and experiments were performed by a blinded investigator. Graphs were generated in Prism 9. Representative images were exported from FIJI and figures were compiled in Inkscape 0.92.4 (Inkscape.org). All data are presented as mean ± SEM unless otherwise stated.

3 | RESULTS

3.1 | An acute systemic 2-DG-induced glucoprivic challenge induced FOS-immunoreactivity in the NTS but did not change GFAP-immunoreactive astrocyte number or morphology

Expression of glial fibrillary-acidic protein (GFAP) by NTS astrocytes is dynamic and greater expression and changes in cellular morphology can be indicative of enhanced activity of these cells.[3,24,28] We injected mice with 2-DG (0.3 g/kg i.p.) and removed food from the cage. Two hours later mice were perfused (Figure 1A). Immunohistochemistry revealed strong induction of the protein product of the immediate early gene *Fos* in the NTS (Figure 1B–D), consistent with previous observations.[20,29] This increase in FOS-immunoreactivity was observed in the postremal NTS with less pronounced differences in the rostral region and no change in caudal sections (Figure 1D). In our experiment, there was no difference between groups in the number of GFAP-immunoreactive cells across the NTS at any of the three rostrocaudal subdivisions examined (Figure 1E). Furthermore, there were no differences in morphological complexity, assessed by Sholl analysis, or mean process number of GFAP-immunoreactive cells between groups (Figure 1F,H). Finally, FOS-immunoreactivity was only very rarely colocalised within GFAP-immunoreactive cells and there were no statistically significant differences in the number of colocalised cells between groups (Figure 1I). Taken together this suggests that at the time point examined, following acute systemic 2-DG-induced glucoprivation, neurons in the postremal NTS were primarily activated without altering GFAP-positive astrocyte cytoskeletal protein immunoreactivity, morphology, or immediate early gene immunoreactivity.

These experiments were performed in both male and female mice and the data stratified by sex are shown in Figure S1. In general, effects were consistent across sexes with the exception of FOS-immunoreactivity in the rostral NTS, which was increased in males injected with 2-DG but not females (Figure S1B,C).

3.2 | Chemogenetic activation of DVC astrocytes suppressed food intake through reduced meal number and size

We sought to characterise hypophagia induced by chemogenetic DVC astrocyte modulation using hM3Dq[24,30] in mice of both sexes by combining this methodology with non-invasive monitoring of food intake, water intake and activity. Mice received bilateral injections of an adeno-associated viral (AAV) vector containing the hM3Dq receptor fused to a fluorescent mCherry reporter under the control of the gfaABC$_1$D GFAP promotor fragment[31] (Figure 2A). This widely used approach drives expression of hM3Dq in astrocytes at the injection site.[32–37] In these mice, mCherry immunoreactivity was consistently observed in the DVC while the degree of extra-DVC transduction varied between mice (Figure 2B,C). At the target injection site (postremal NTS) mCherry-immunoreactivity was observed associated with 85.72 ± 5.4% of GFAP-immunoreactive cells ($n = 3$ mice, 1 section per mouse) in a diffuse pattern consistent with a membrane-bound protein (Figures 2D and S2A).[38,39] Of note, GFAP-immunoreactivity was not observable in all DVC astrocytes and some areas had sparse labelling. We found that the mCherry-immunoreactivity was largely overlapping with S100B, a marker of the astrocyte cytoplasm which more robustly labelled astrocytes throughout the DVC (Figure S2B). In the same area, mCherry-immunoreactivity was absent from NeuN-immunoreactive cells (0.00 ± 0.00%, $n = 3$ mice, 1 section per mouse), (Figures 2E and S2C) and virally labelled glutamatergic neurons (Vglut2-IRES-Cre mice coinjected with AAV-hSyn-DIO-Egfp, Figure S2D). Subsequently, we refer to mice injected with AAV-hGFAP-hM3Dq_mCherry in the DVC as DVC::GFAP^{hM3Dq} mice.

DVC::GFAP^{hM3Dq} mice were injected i.p. with either saline or CNO (1 mg/kg) immediately prior to the onset of the dark phase, and food intake, water intake and physical activity continually remotely monitored for the following 23 h. Injection with CNO reduced cumulative food intake in female and male mice during this period relative to when the same mice received saline injection (Figure 2F,J). Analysis of the rate of food intake shows this effect was most pronounced during the first 6 h of the dark phase (Figure 2G,K). Analysis of meal patterning showed no statistically significant changes in the number of meals eaten during the dark phase although in both sexes there was a trend towards a reduced meal number following CNO injection (Figure 2H,L). Similarly, the average size of a meal was smaller following injection with CNO when compared with saline (Figure 2I,M); however, this only reached statistical significance in females. Since both patterning parameters trended lower after CNO injection it suggests that these factors additively contribute towards the reduction in food intake. Thus, chemogenetic activation of DVC astrocytes suppressed food intake by reducing hunger (fewer meals initiated) and advancing satiety (initiated meals are smaller).

Water intake was also reduced on CNO injection days as compared with saline (Figures S3A,C). Similarly, activity measured by the cumulative number of beam break events was reduced by injection with CNO relative to saline (Figures S3B,D). As water intake and activity (food seeking) are linked to feeding, from our experiment it is unclear whether these effects are secondary to reduced food intake or driven by distinct mechanisms.

In parallel, we tested mice injected with AAV-GFAP-mCherry and therefore lacking the hM3Dq receptor. In this group, treatment with CNO had no effect on food intake, meal patterning or water intake but did induce a slight, statistically significant, decrease in total activity (Figure S4).

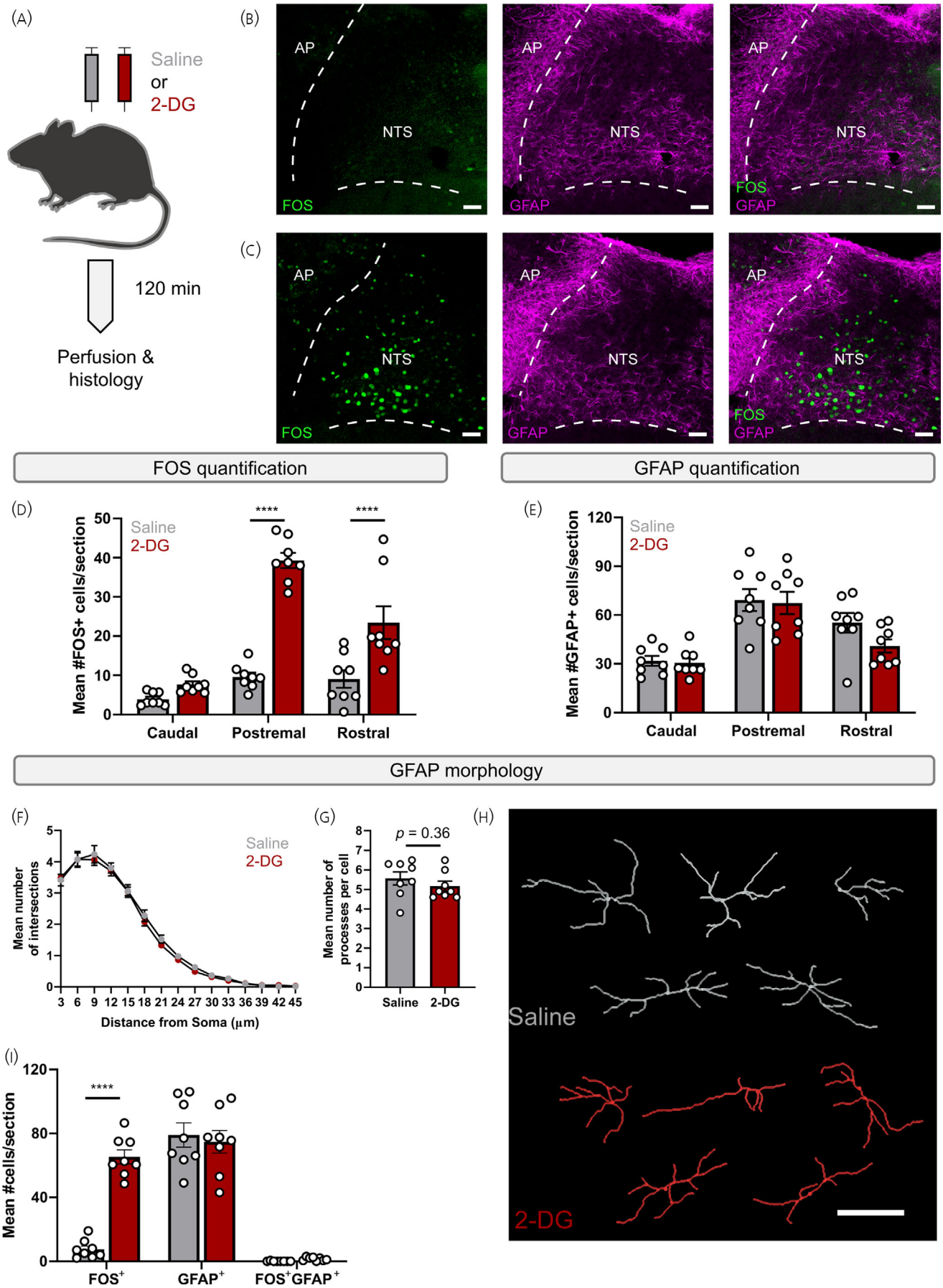

FIGURE 1 Legend on next page.

3.3 | Chemogenetic activation of DVC astrocytes suppressed glucoprivic feeding

We reasoned that if they are indeed primary detectors of low glucose, chemogenetic activation of DVC astrocytes may enhance the subsequent homeostatic physiological responses. If so, this could occur by enhancing glucoprivic feeding, elevating basal blood glucose, promoting absorption of glucose from the blood, and/or ameliorating insulin-induced hypoglycaemia.

To test the effect of DVC astrocyte activation on glucoprivic feeding, DVC::GFAP^{hM3Dq} mice were injected i.p. with saline or CNO (1 mg/kg) during the light phase. Then, 30 min later mice were injected i.p. with either saline or 2-DG (0.4 g/kg) and food intake was measured from this time point (Figure 3A). Since the observed effects were consistent across sexes, data were pooled (data are shown separated by sex in Figure S5). In line with other studies,[25] in the absence of chemogenetic activation of DVC astrocytes, i.p. 2-DG treatment increased food intake at 2, 4 and 8 h compared to injection with saline (Figure 3B). In contrast to our hypothesis, injection with CNO prior to 2-DG attenuated glucoprivic feeding to levels equivalent to injection with saline alone (Figure 3B). This indicates that glucoprivic feeding is suppressed by chemogenetic activation of DVC astrocytes.

At 24 h after injection, compared to saline treated controls, there was no longer a statistically significant effect of 2-DG treatment on food intake measurements in DVC::GFAP^{hM3Dq} mice (Figure 3B). However, CNO-treatment in DVC::GFAP^{hM3Dq} mice resulted in a statistically significant reduction in 24 h food intake compared to saline treatment regardless of whether 2-DG was also administered (Figure 3B). This is consistent with our feeding data (Figure 2G,K) where the rate of food intake is reduced for ~12 h after CNO injection before returning to normal. In these studies and our prior studies of fast-induced refeeding[24] we did not see a compensatory increase in food intake following the offset of CNO's presumed effect window.

A control group of DVC::GFAP^{mCherry} mice showed that CNO alone did not suppress glucoprivic feeding (Figure S6). We did, however, find a statistically significant increase in food intake in CNO injected DVC::GFAP^{mCherry} mice compared with saline alone 8 and 24 h after injection (Figure S6). Since we have not observed this previously (Figure S4) it is possible this finding is spurious.[24] Additionally, the direction of this finding is opposite to our observation of food intake suppression in DVC::GFAP^{hM3Dq} mice therefore CNO alone does not account for our findings.

3.4 | Chemogenetic activation of DVC astrocytes was not sufficient to alter basal blood glucose levels

We next assessed the effects of chemogenetic activation of DVC astrocytes on blood glucose levels. Chemogenetic activation of GABAergic DVC neurons is sufficient to elevate blood glucose via modulation of hepatic glucose production,[13] likely part of the defensive mechanisms against hypoglycaemia. To test whether this mechanism is engaged by chemogenetic activation of DVC astrocytes, blood glucose levels were measured from a cut in the tail 30 min after i.p. injection with saline or CNO. Neither female nor male DVC::GFAP^{hM3Dq} mice showed a statistically significant difference between treatments (Figure 4A,E). Of note, these values are pooled from glucose and insulin tolerance tests (see below) and are therefore corrected for multiple comparisons. These data suggest that, at the time-point tested, chemogenetic activation of DVC astrocytes alone was not sufficient to initiate mechanisms to increase blood glucose.

3.5 | Chemogenetic activation of DVC astrocytes showed potential sex-dependent effects in the glucose tolerance test

Chemogenetic activation of some DVC neurons (identified by expression of either preproglucagon [PPG] or choline acetyltransferase [ChAT]) can improve glucose clearance from the blood following a bolus glucose injection in a glucose tolerance test.[40,41] We tested whether chemogenetic activation of DVC astrocytes was sufficient to recapitulate this effect, potentially via these downstream neurons. In female mice, blood glucose was lower 15 min following i.p. injection with glucose in CNO-injected tests when compared to saline-injected tests (Figure 4B). This effect appeared to be specific to the initial

FIGURE 1 Systemic glucoprivation induced nucleus of the solitary tract (NTS) FOS-immunoreactivity (IR) but did not change the number of glial fibrillary acidic protein (GFAP)-immunoreactive cells or their morphology. (A) Schematic of experimental design ($n = 8$ mice per group, 5 male, 3 female). (B) Representative image of FOS- and GFAP-immunoreactivity in the NTS of a saline-injected mouse. (C) Representative image of FOS- and GFAP-immunoreactivity in the NTS of a 2-deoxyglucose (2-DG) (0.3 g/kg i.p.) injected mouse. (D) Quantification of the number of FOS cells across the rostrocaudal extent of the NTS (two-way analysis of variance [ANOVA] with Sidak's post hoc test; $p_{treatment}$ <0.0001 $F_{(1,42)} = 80.17$, $p_{rostro\text{-}caudal\ position}$ < 0.0001 $F_{(2,42)} = 38.87$, $p_{interaction}$ <0.0001 $F_{(2,42)} = 17.98$). (E) Quantification of the number of GFAP-immunoreactive cells across the rostrocaudal extent of the NTS (two-way ANOVA with Sidak's post hoc test; $p_{treatment} = 0.18$ $F_{(1,42)} = 1.86$, $p_{rostro\text{-}caudal\ position}$ < 0.0001 $F_{(2,42)} = 25.34$, $p_{interaction} = 0.38$ $F_{(2,42)} = 1.0$). (F) Mean Sholl profile of GFAP-immunoreactive cells in the NTS ($n = 8$ mice per group, 5 male, 3 female. One value calculated per animal as the mean of 10 randomly selected astrocytes. Two-way ANOVA with Sidak's post hoc test; $p_{treatment} = 0.19$ $F_{(1,210)} = 1.80$, $p_{distance}$ < 0.0001 $F_{(14,210)} = 339.3$, $p_{interaction} = 0.99$ $F_{(14,210)} = 0.25$). (G) Mean number of processes of GFAP-immunoreactive cells in the NTS ($n = 8$ mice per group, 5 male, 3 female. One value calculated per animal as the mean of 10 randomly selected astrocytes. Unpaired *t*-test). (H) Representative traces of five cells from a saline- (top row, grey) or 2DG- (bottom row, red) injected mouse. (I) Quantification of the number of cells immunoreactive for FOS, GFAP or both in the postremal NTS (two-way ANOVA with Sidak's post hoc test; $p_{treatment}$ < 0.0001 $F_{(1,42)} = 23.08$, p_{target} <0.0001 $F_{(2,42)} = 133.1$, $p_{interaction}$ <0.0001 $F_{(2,42)} = 27.03$). Scale bar = 50 μm (B, C), 10 μm (H). **** = p < .0001.

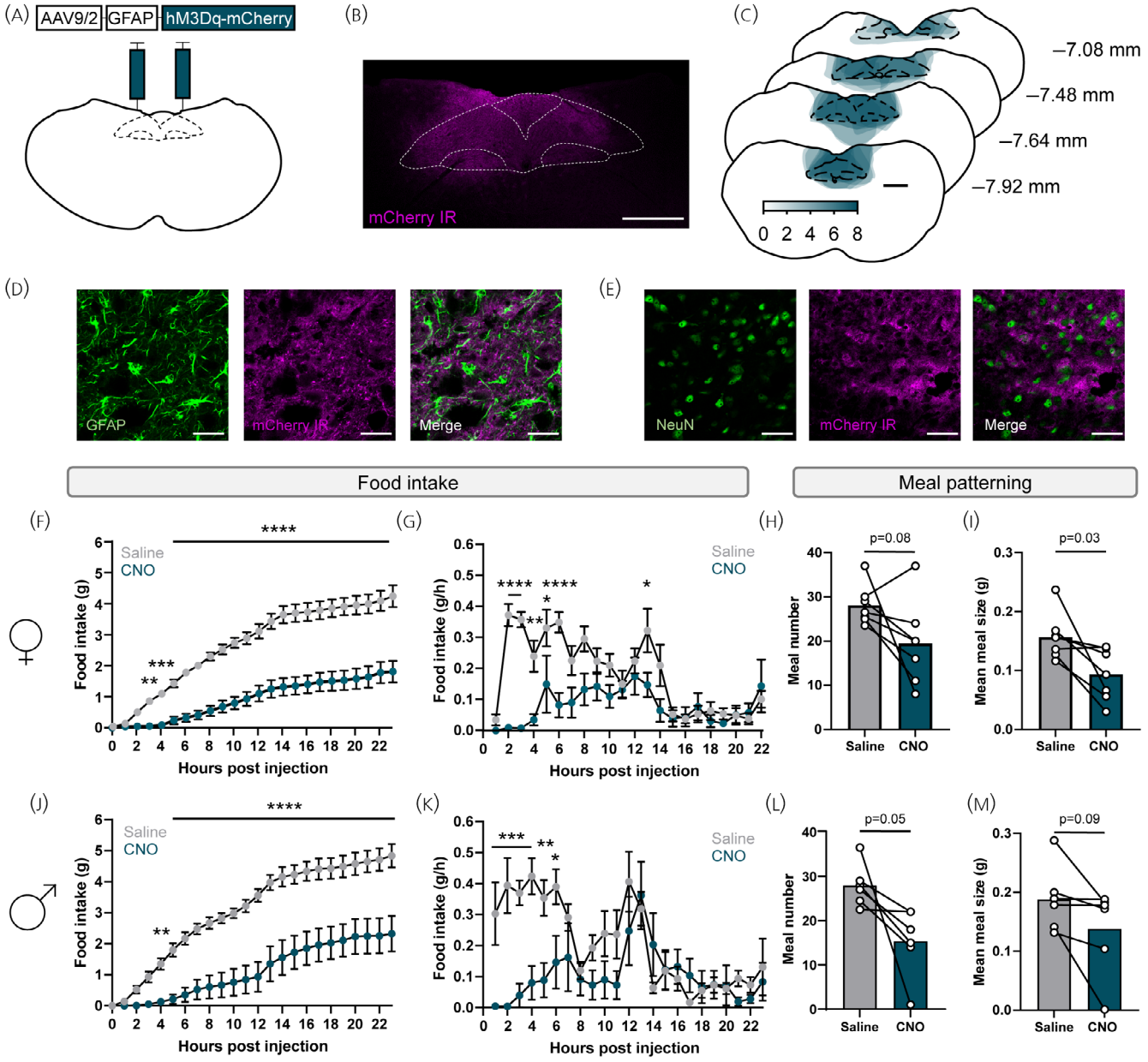

FIGURE 2 Chemogenetic activation of dorsal vagal complex (DVC) astrocytes reduced food intake in male and female mice. (A) Schematic of viral vector delivery. (B) Representative mCherry-immunoreactivity (IR) following viral vector injection. (C) Quantification of mCherry-IR area ($n = 8$ mice, 5 female, 3 male). (D) Spatial association of GFAP- and mCherry-IR in the DVC. (E) Spatial separation of NeuN and mCherry-IR in the DVC. (F) Cumulative food intake of female DVC::GFAP^{hM3Dq} mice ($n = 7$, all panels) following injection with saline (grey) or CNO (blue) (two-way repeated measures analysis of variance [RM ANOVA] with Sidak's post hoc test; $p_{treatment} = 0.0025$ $F_{(1,6)} = 40.39$, $p_{time} < 0.0001$ $F_{(23,138)} = 154.1$, $p_{interaction} < 0.0001$ $F_{(23,138)} = 11.95$). (G) Food intake rate of female DVC::GFAP^{hM3Dq} mice following injection with saline (grey) or CNO (blue) (two-way RM ANOVA with Sidak's post hoc test; $p_{treatment} < 0.007$ $F_{(1,6)} = 16.11$, $p_{time} < 0.0001$ $F_{(21,126)} = 7.13$, $p_{interaction} < 0.0001$ $F_{(21,126)} = 4.71$). (H) Meal number of female DVC::GFAP^{hM3Dq} mice following injection with saline (grey) or CNO (blue) (paired *t*-test). (I) Meal size of female DVC::GFAP^{hM3Dq} mice following injection with saline (grey) or CNO (blue) (paired *t*-test). (J) Cumulative food intake of male DVC::GFAP^{hM3Dq} mice ($n = 6$, all panels) following injection with saline (grey) or CNO (blue) (two-way RM ANOVA with Sidak's post hoc test; $p_{treatment} = 0.012$ $F_{(1,5)} = 14.88$, $p_{time} < 0.0001$ $F_{(23,115)} = 81.49$, $p_{interaction} < 0.0001$ $F_{(23,115)} = 7.59$). (K) Food intake rate of male DVC::GFAP^{hM3Dq} mice following injection with saline (grey) or CNO (blue) (two-way RM ANOVA with Sidak's post hoc test; $p_{treatment} = 0.02$ $F_{(1,5)} = 11.09$, $p_{time} < 0.0001$ $F_{(21,105)} = 3.57$, $p_{interaction} < 0.0001$ $F_{(21,105)} = 4.97$). (L) Meal number of male DVC::GFAP^{hM3Dq} mice following injection with saline (grey) or CNO (blue) (paired *t*-test). (M) Meal size of male DVC::GFAP^{hM3Dq} mice following injection with saline (grey) or CNO (blue) (paired *t*-test). Scale bar = 500 μm (B, C), 25 μm (D, E). * = $p < .05$, ** = $p < .01$, *** = $p < .001$, **** = $p < .0001$.

elevation in blood glucose since there were no statistically significant differences at any other time points (Figure 4B) nor in the baseline-subtracted area under the curve (Figure 4C). In male mice, however, there were no statistically significant effects of CNO treatment on the blood glucose levels observed at any time point assessed (Figure 4F), or across the entire test, measured by baseline-subtracted area under

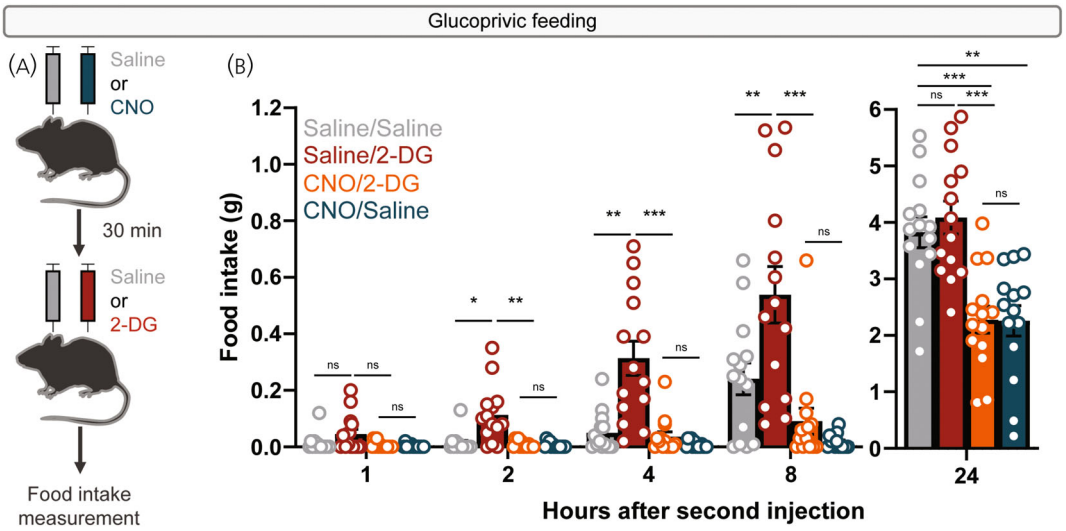

FIGURE 3 Chemogenetic activation of dorsal vagal complex (DVC) astrocytes attenuated glucoprivic feeding in mice of both sexes. (A) Schematic of experimental protocol. (B) Cumulative food intake of mice injected with saline or clozapine-*N*-oxide (CNO) followed by saline or 2-deoxyglucose (2-DG) ($n = 14$ mice, 7 female, 7 male, two-way repeated measures analysis of variance [RM ANOVA] with Geisser–Greenhouse correction, Sidak's post hoc test; $p_{treatment} < 0.0001$ $F_{(2.67,34.74)} = 30.40$, $p_{time} < 0.0001$ $F_{(1.079,14.03)} = 257.9$, $p_{interaction} < 0.0001$ $F_{(2.37,30.86)} = 16.99$). * = $p < .05$, ** = $p < .01$, *** = $p < .001$, **** = $p < .0001$. n.s., not statistically significant.

the curve (Figure 4G). The effect in female mice possibly indicates more rapid glucose clearance or enhanced first-phase insulin secretion.

Due to the divergent effect of CNO between sexes (Figure 4B,F) data for all blood glucose measurements were stratified by sex rather than pooled as for other data.

3.6 | Chemogenetic activation of DVC astrocytes was not sufficient to alter glucose homeostasis responses in the insulin tolerance test

Finally, we tested whether chemogenetic activation of DVC astrocytes altered the response to subsequent insulin-induced hypoglycaemia in the insulin tolerance test. We hypothesised that increasing DVC astrocyte activity would be protective against this stimulus by reducing the severity of hypoglycaemia and/or improving blood glucose recovery by stimulating hepatic glucose production.[13] In contrast to our hypothesis, at the time points assessed no difference was observed in the response to insulin-induced hypoglycaemia between saline or CNO injection in female or male DVC::GFAP^{hM3Dq} mice, neither in the initial reduction in blood glucose nor subsequent recovery (Figure 4D,H).

Taken together, the results from the glucose homeostasis assessments suggest that activation of DVC astrocytes was not sufficient to modulate basal blood glucose nor was it protective against subsequent insulin-induced hypoglycaemia. There was, however, a statistically significant reduction in the peak glucose excursion in female mice during the glucose tolerance test.

In parallel, we performed all experiments evaluating glucose homeostasis parameters in control DVC::GFAP^{mCherry} mice and observed no statistically significant effects of CNO on basal blood glucose, glucose tolerance or insulin tolerance (Figure S7).

3.7 | Chemogenetic activation of DVC astrocytes did not selectively activate catecholaminergic NTS neurons

We previously observed that chemogenetic activation of DVC astrocytes induced FOS-immunoreactivity in the DVC and lateral parabrachial nucleus.[24] In the current study we sought to identify whether NTS catecholaminergic neurons, identified by their expression of TH (NTSTH neurons), were among those recruited, perhaps being selectively recruited over non-catecholaminergic NTS neurons. This neuronal population was specifically selected for study as NTSTH neurons are involved in both appetite suppression and glucoprivic feeding in mice.[12,42] Additionally, DVC astrocytes increase $[Ca^{2+}]_i$ of NTSTH neurons by a purinergic mechanism under low glucose conditions in brain slices.[18]

DVC::GFAP^{hM3Dq} and DVC::GFAP^{mCherry} mice were injected with CNO and food removed from the cage 2 h prior to perfusion. Dual-immunohistochemistry was subsequently performed to identify NTSTH neurons and FOS-immunoreactivity (Figure 5A,B). As we observed previously, following CNO treatment there were more FOS-immunoreactive cells in the NTS of DVC::GFAP^{hM3Dq} mice compared with DVC::GFAP^{mCherry} controls (Figure 5C). There was a statistically significant difference in the percentage of NTSTH neurons containing FOS-immunoreactivity between groups (Figure 5D), which was most pronounced in the postremal and rostral sections. Relative to the whole NTSTH population, 27% of NTSTH neurons of DVC::GFAP^{hM3Dq} mice had FOS-immunoreactivity, compared with 7% in DVC::

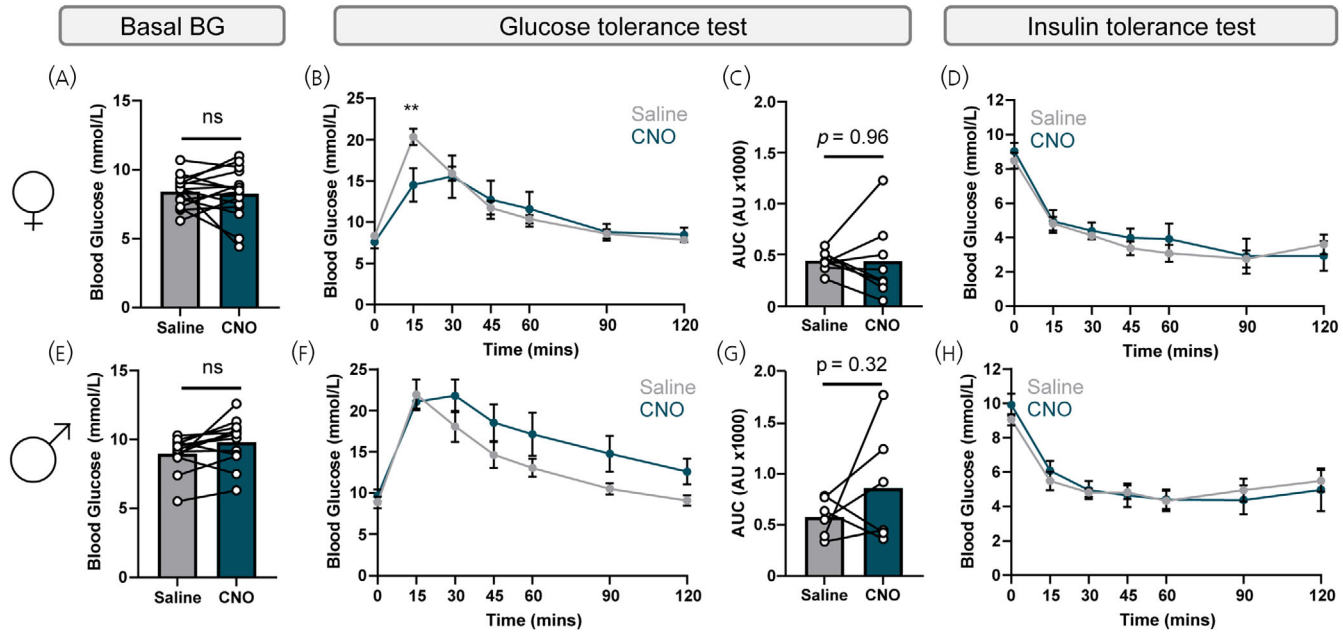

FIGURE 4 Chemogenetic activation of dorsal vagal complex (DVC) astrocytes suppressed initial glucose-induced hyperglycaemia in female mice but not males (A) Basal blood glucose (BG) measured 30 min after injection with saline (grey) or clozapine-*N*-oxide (CNO) (blue) ($n = 15$ female mice, paired *t*-test with Bonferroni correction). (B) Glucose tolerance curve of mice injected with saline (grey) or CNO (blue) ($n = 8$ female mice, two-way repeated measures analysis of variance [RM ANOVA] with Sidak's post hoc test; $p_{treatment} = 0.66$ $F_{(1,7)} = 0.21$, $p_{time} < 0.0001$ $F_{(6,42)} = 25.37$, $p_{interaction} < 0.0001$ $F_{(6,42)} = 6.24$). (C) Baseline subtracted area under the curve (AUC) for glucose tolerance test in mice injected with saline (grey) or CNO (blue) ($n = 8$ female mice, paired *t*-test). (D) Insulin tolerance curve of mice injected with saline (grey) or CNO (blue) ($n = 7$ female mice, two-way ANOVA with Sidak's post hoc test; $p_{treatment} = 0.69$ $F_{(1,6)} = 0.18$, $p_{time} < 0.0001$ $F_{(6,36)} = 40.06$, $p_{interaction} = 0.59$ $F_{(6,36)} = 0.78$). (E) Basal blood glucose (BG) measured 30 min after injection with saline (grey) or CNO (blue) ($n = 13$ male mice, paired *t*-test with Bonferroni correction). (F) Glucose tolerance curve of mice injected with saline (grey) or CNO (blue) ($n = 6$ male mice, two-way RM ANOVA with Sidak's post hoc test; $p_{treatment} = 0.21$ $F_{(1,5)} = 2.02$, $p_{time} < 0.0001$ $F_{(6,30)} = 47.51$, $p_{interaction} = 0.21$ $F_{(6,30)} = 1.52$). (G) Baseline subtracted area under the curve (AUC) for glucose tolerance test in mice injected with saline (grey) or CNO (blue) ($n = 6$ male mice, paired *t*-test). (H) Insulin tolerance curve of mice injected with saline (grey) or CNO (blue) ($n = 7$ male mice, two-way ANOVA with Sidak's post hoc test; $p_{treatment} = 0.89$ $F_{(1,6)} = 0.02$, $p_{time} < 0.0001$ $F_{(6,36)} = 24.89$, $p_{interaction} = 0.54$ $F_{(6,36)} = 0.86$). * = $p < .05$, ** = $p < .01$, *** = $p < .001$.

GFAP^{mCherry} mice. In addition, we observed many FOS-immunoreactive cells that did not express TH (Figure 5E). This indicates that although there is some recruitment of NTSTH neurons by chemogenetic DVC astrocyte activation this represents a minority of NTSTH neurons. Furthermore, since far more non-TH neurons are activated, there appears to be no preferential recruitment of NTSTH neurons by this manipulation.

4 | DISCUSSION

In this study we set out to determine the ability of astrocytes in the NTS and wider DVC to sense acute systemic 2-DG-induced glucoprivation, and whether their chemogenetic activation was sufficient to modulate glucose homeostasis. We found that NTS GFAP-expressing astrocytes did not increase their FOS-immunoreactivity following acute systemic 2-DG treatment nor did they alter their primary process morphology. Furthermore, the number of GFAP-expressing cells in the NTS was equivalent between groups. In addition, we verified that chemogenetic activation of DVC astrocytes cells suppressed nocturnal food intake in mice of both sexes, and attenuated glucoprivic feeding following systemic 2-DG administration. We found no effect of chemogenetic stimulation of DVC astrocytes on systemic glucose homeostasis in male mice as assessed by the glucose and insulin tolerance tests. During the glucose tolerance tests, female mice showed a lower peak blood glucose 15 min following injection with glucose in CNO-injected tests when compared to saline-injected tests. These mice showed no differences in the blood glucose profile following CNO or saline treatment in the insulin tolerance tests. Finally, we observed that chemogenetic activation of DVC astrocytes subsequently activates a small number of NTSTH neurons, but these represent a minor proportion of both total NTSTH neurons and total FOS-immunoreactive cells, suggesting NTSTH neurons are not selectively activated.

4.1 | NTS astrocytes did not show signs of morphological change following an acute systemic 2-DG-induced glucoprivic challenge

In rodent brain slices, NTS astrocytes have been demonstrated to respond directly to both glucoprivation and hormones/hormone

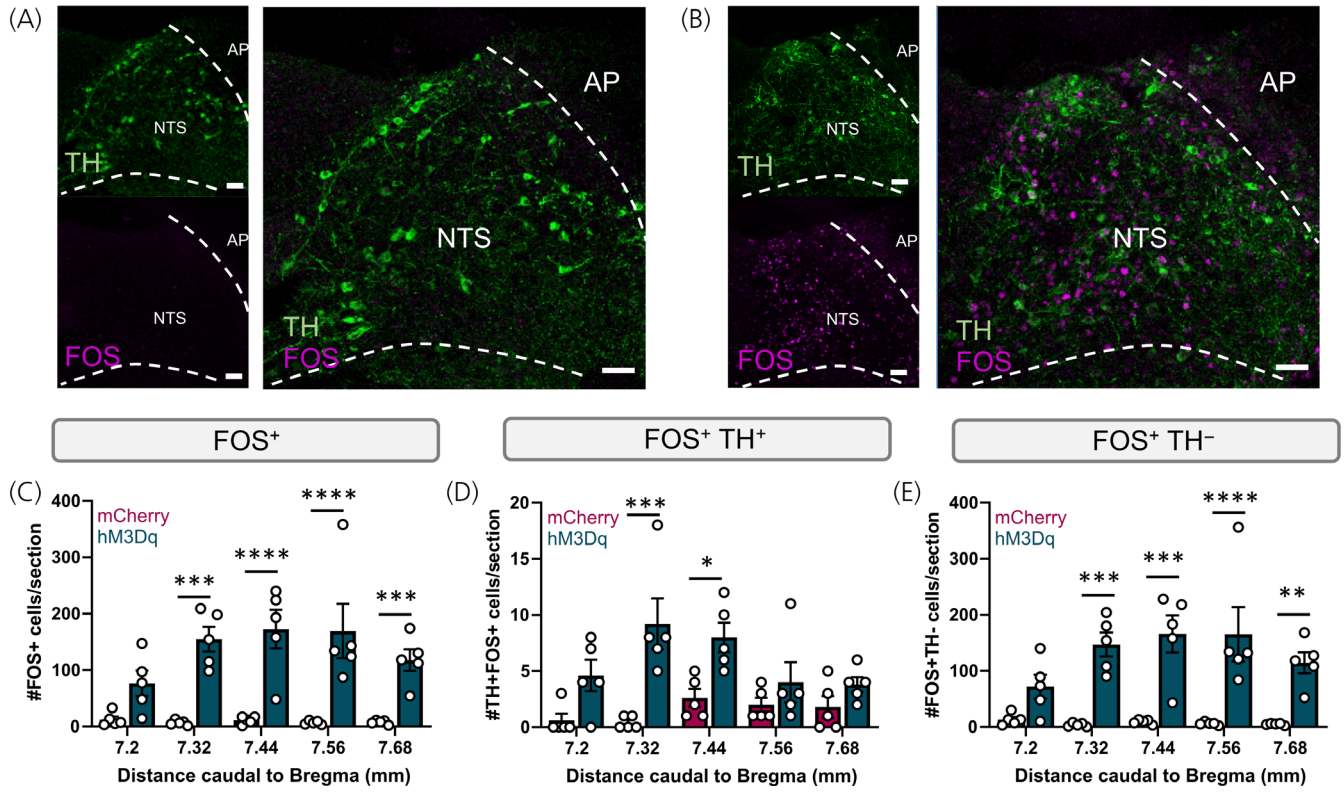

FIGURE 5 Chemogenetic activation of dorsal vagal complex (DVC) astrocytes predominantly recruited non-catecholaminergic neurons. (A) Representative image of tyrosine hydroxylase (TH) and FOS-immunoreactivity (IR) in the nucleus of the solitary tract (NTS) of DVC::GFAP^{mCherry} mice injected with clozapine-*N*-oxide (CNO). (B) Representative image of TH and FOS-IR in the NTS of DVC::GFAP^{hM3Dq} mice injected with CNO. (C) Quantification of FOS-IR cells in the NTS of DVC::GFAP^{mCherry} and DVC::GFAP^{hM3Dq} mice injected with CNO ($n = 5$ mice per group, 2 female, 3 male. Two-way analysis of variance [ANOVA] with Sidak's post hoc test; $p_{treatment}$ <0.0001 $F_{(1,40)} = 85.66$, $p_{rostrocaudal\ position} = 0.19$ $F_{(4,40)} = 1.60$, $p_{interaction} = 0.15$ $F_{(4,40)} = 1.81$). (D) Percentage of TH cells coexpressing FOS-IR in the NTS of DVC::GFAP^{mCherry} and DVC::GFAP^{hM3Dq} mice injected with CNO ($n = 5$ mice per group, 2 female, 3 male. Two-way ANOVA with Sidak's post hoc test; $p_{treatment}$ <0.0001 $F_{(1,40)} = 24.44$, $p_{rostrocaudal\ position} = 0.85$ $F_{(4,40)} = 0.34$, $p_{interaction} = 0.54$ $F_{(4,40)} = 0.79$). (E) Quantification of FOS-IR cells lacking TH-IR in the NTS of DVC::GFAP^{mCherry} and DVC::GFAP^{hM3Dq} mice injected with CNO ($n = 5$ mice per group, 2 female, 3 male. Two-way ANOVA with Sidak's post hoc test; $p_{treatment}$ <0.0001 $F_{(1,40)} = 83.20$, $p_{rostrocaudal\ position} = 0.22$ $F_{(4,40)} = 1.51$, $p_{interaction} = 0.13$ $F_{(4,40)} = 1.89$). * = $p < .05$, ** = $p < .01$, *** = $p < .001$**** = $p < .0001$.

receptor ligands that alter systemic glucose homeostasis and food intake.[16–18,21,43,44] However, in our experiment, we did not find evidence of morphological reorganisation or an increased number of GFAP-immunoreactive cells following acute systemic 2-DG-induced glucoprivation. This is one piece of evidence and does not rule out other cellular changes occurring in these cells in response to in vivo 2-DG treatment. A limitation of this study is that we did not confirm changes in DVC astrocyte Ca^{2+} using any experimental modality following systemic 2-DG or CNO. In prior work, we have demonstrated that chemogenetic stimulation via hM3Dq is sufficient to induce morphological changes in GFAP-expressing cells[24] and others have shown that chemogenetic stimulation of astrocytes via hM3Dq increases intracellular Ca^{2+} responses.[33] Astrocytes may well show Ca^{2+} fluctuations resolvable in slice imaging that do not lead to the downstream cellular changes assessed in this study, that is, GFAP or FOS expression, or morphological reorganisation. In the published brain slice experiments only a proportion (~40%) of NTS astrocytes respond to glucoprivation,[18] so it is possible that we did not detect an effect if it was "diluted" by non-responsive astrocytes. Both astrocyte metabolism and purinergic transmission are required for hyperglycaemia induced by subcutaneous 2-DG administration in anaesthetised rats,[19] and while this suggests a primary sensory role for astrocytes, an alternative explanation could be that homeostatic functions of astrocytes, which maintain synaptic transmission in the NTS,[3] are necessary, but not sufficient, for glucose-sensing neurons to mount appropriate physiological responses to rectify deviations from euglycemia.

The time-course we used in our immunohistochemistry experiments (perfusion 2 h after intraperitoneal injection of 2-DG) is shorter than in our previous studies, which detected a morphological change in NTS astrocytes following 12 h of high-fat high-sucrose diet intake.[24] This time point for perfusion was chosen to maximise FOS-immunoreactivity which decays over longer periods of time, and to limit the contribution of secondary responses (e.g., endocrine responses to 2-DG induced hyperglycaemia). Therefore, while it is certainly possible that at later points morphological changes may be

visible, other studies report rapid reorganisation of astrocyte morphology by food intake or hormone administration in the order of 1–2 h, albeit using different methodology (electron microscopy).[45,46] Additionally, we only examined the morphology of the primary processes (visualised by GFAP immunoreactivity) which does not label the fine processes that make up much of the astrocyte cell volume.[47] As such it is certainly possible that the morphology of these finer processes may change, altering the proximity of the astrocyte to neuronal synapses and modulating transmission as a result.

In order to unify our findings with brain slice imaging, in vivo recording of astrocyte Ca^{2+} with fibre photometry or imaging is a promising future direction.[48] Due to the location of the DVC below the craniovertebral junction there are significant technical challenges associated with doing this in awake freely moving mice, although recently fibre photometry recordings have been published for both astrocytes in the striatum and neurons in the NTS.[49,50] As such, it is possible that combining these approaches may reveal the real-time responses of astrocytes to deviations in energy status in intact animals which were not evident using the approach employed here.

4.2 | Chemogenetic activation of DVC astrocytes suppressed food intake even under glucoprivic conditions

While chemogenetic activation of DVC astrocytes suppresses food intake under conditions of physiological hunger (12 h overnight fast),[24] fast-induced food intake and glucoprivic feeding are functionally separable at the circuit level.[51] Despite this distinction, chemogenetic DVC astrocyte activation suppressed 2-DG induced food intake to levels comparable with saline injection. This suggests that the activation of appetite suppressing neurons downstream of these astrocytes likely occludes or overrides signals of glucoprivation. Indeed, when we examined using immunohistochemistry the cell types activated following DVC astrocyte stimulation only a minority were NTS^{TH} cells, a subpopulation of which have been reported to drive glucoprivic feeding.[5,12] Thus, the net effect of broad chemogenetic activation of DVC astrocytes is to suppress food intake. However, these results do not rule out the possibility that subsets of DVC astrocytes are specialised for sensing glucoprivation and preferentially communicate with the appropriate neurons to drive responses that restore glucose homeostasis. Further research into the heterogeneity of astrocytes[52] may reveal markers that allow selective targeting of subpopulations for manipulation and/or monitoring.

Chemogenetic activation of astrocytes evokes increases in intracellular Ca^{2+} mediated by Gq-coupled second messengers.[35] This resembles endogenous intracellular signalling pathways and leads to downstream effects on neuronal activity. NTS astrocytes have receptors for and/or have been demonstrated to increase their intracellular Ca^{2+} in response to numerous stimuli relevant to physiological control of food intake and blood glucose control including vagal afferent stimulation,[53,54] appetite regulating hormones[43,44,55] and circulating factors.[56] Thus, it is possible that this manipulation recapitulates some aspects of the endogenous astrocyte activity evoked by these stimuli. Loss of function experiments and real-time activity measurements (discussed above) would reveal the response of astrocytes to these cues and the contribution of this signalling to the effects of hormones and/or vagal inputs.

The possibility that the impact of bulk chemogenetic activation of DVC astrocytes on food intake (both nocturnal and glucoprivic) is mediated, at least in part, via activation of nausea-associated neural pathways, still cannot be excluded as hindbrain circuits controlling feeding are associated with both aversive and non-aversive responses (for review see[57]). However, there is strong precedence in the literature, including from data in rodent studies examining cholecystokinin (CCK[58]), prolactin-releasing peptide (PrRP[59]) and glucagon-like peptide-1 (GLP-1[60,61]) signalling, indicating that aversion per se is not necessarily non-physiological as satiety and nausea/malaise are likely on the same physiological continuum. A recent study by Clyburn and colleagues showed that chemogenetic (GFAP-hM4DGi) or pharmacological (fluoroacetate) mediated inhibition of astrocytes in the rat dorsal DMV prolongs high-fat diet induced hyperphagia during the initial homeostatic adjustment to the diet by modulating glutamatergic signalling, resulting in alterations in gastric emptying.[62] While this study focuses on inhibition of DMV astrocyte activity, it supports the notion that specific modulation of these cells in the DVC is sufficient to physiologically impact feeding. In agreement with our data, they observed that in control viral vector injected rats CNO treatment (either 1 mg/kg or 3 mg/kg i.p.) alone is not sufficient to reduce food intake.

4.3 | Chemogenetic activation of DVC astrocytes had a sex-specific effect on glucose homeostasis in the glucose tolerance test

Using chemogenetic activation we uncovered that astrocytes may facilitate glucose clearance in female mice. Due to the short onset and duration of this effect (which was only evident at 15 min post-glucose injection) it is possible that it is mediated by enhanced first-phase glucose-stimulated insulin secretion, although direct measurements of plasma insulin are required to confirm this. This suggests a state-dependence of the effect since, prior to injection of glucose, CNO had no effect on blood glucose compared to saline. Interestingly, this is contrary to our predictions made based on loss-of-function experiments showing a dependence on intact DVC astrocyte activity for subsequent 2-DG-induced elevations in blood glucose.[19] Together, our findings combined with previous work by others suggest that activity of DVC astrocytes is necessary but not sufficient for these elevations in blood glucose. Similarly, the published astrocyte-dependent compensatory increase in blood glucose in response to glucoprivation in the anaesthetised rat suggests that activation of astrocytes may be protective against hypoglycaemia;[19] however, in our study in freely moving mice we found this was not the case, again potentially supporting necessity but not sufficiency of DVC astrocytes for this effect.

In our glucose homeostasis studies, chemogenetic activation of DVC astrocytes was performed 30 min prior to manipulation of

systemic glucose with intraperitoneal administration of 2-DG (glucoprivic feeding), glucose (glucose tolerance test), or insulin (insulin tolerance test). In line with the postulate that the DVC astrocytes may be among the first responding cells in this region, this study addressed whether chemogenetic activation of DVC astrocytes was sufficient to alter blood glucose and/or the response to subsequent challenges to glucose homeostasis. Whether chemogenetic activation of DVC astrocytes can alter the physiological responses during the homeostatic challenge, for example, administering 2-DG, glucose, or insulin followed by CNO in DVC::GFAP^{hM3Dq} mice is unknown. This could reveal whether astrocytes may have different roles and responses in distinct metabolic states and should be the subject of future studies.

4.4 | Uncovering neural circuits downstream of chemogenetic stimulation of DVC astrocytes

Using immunohistochemistry, we examined whether TH neurons were preferentially recruited following chemogenetic activation of DVC astrocytes. Instead, we found that the most FOS-immunoreactivity was in TH-negative cells. The percentage of NTSTH neurons that were activated increased in more rostral sections relative to caudal. At these levels, there are NTSTH neurons that both stimulate and inhibit feeding[63] and so it is possible that more feeding-suppressive than feeding-stimulating neurons are recruited. Communication between astrocytes and neighbouring neurons induced by this manipulation may be non-random which raises the question of which neuronal populations are expressing FOS. From our functional data we can speculate that PPG, ChAT and GABA neurons are not recruited since the published effects of chemogenetic manipulation of these cells on blood glucose and glucose tolerance[13,40,41] were not recapitulated in our studies, although further investigation is required to confirm this assertion. It is also, however, possible that one or more of these neuronal populations are recruited non-selectively and their actions occlude one another or are diluted by bulk CNO-induced NTS neuronal activation in our experiment.

Building on our published work in male mice,[24] following chemogenetic stimulation of DVC astrocytes, we found food intake was reduced in both male and female animals associated with both reduced meal size and frequency. We previously observed FOS-immunoreactivity in the lateral parabrachial nucleus after chemogenetic stimulation of DVC astrocytes.[24] Together, these findings suggest that the activated neurons are likely glutamatergic since these neurons account for all appetite suppressing NTS subtypes[64] and NTS projections to the lateral parabrachial nucleus have been observed to be glutamatergic.[42,65]

5 | CONCLUSION

We initially posited that DVC astrocytes could be primary glucoprivation sensors, whose activation alone is sufficient to stimulate counter-regulatory circuitry and downstream glucose homeostasis responses, but this was not supported by our experimental observations using bulk chemogenetic activation of astrocytes across the mouse DVC. Superficially, this appears to contrast with the published data indicating that DVC astrocytes can detect low glucose in ex vivo rat brain slices[16–18] and that pharmacologically inhibiting their activity prevents 2-DG-induced compensatory hyperglycaemia in anaesthetised rats.[19] This may potentially be accounted for by a divergence of necessity (as suggested by published studies looking at pharmacological inhibition) and sufficiency (as suggested by our studies herein looking at chemogenetic activation). However, the picture is likely far more complex with regional and physiological state-dependent differences in astrocyte function influencing their roles in brainstem circuity. As stated above, the results presented here do not rule out the possibility that subsets of DVC astrocytes are specialised for sensing glucoprivation by virtue of their location and/or unique functional capabilities, and that these preferentially communicate with the appropriate neurons to drive responses that restore glucose homeostasis. This is supported by data from the rat brain slice experiments showing that only a proportion (~40%) of NTS astrocytes respond to glucoprivation.[18] Within the brainstem, neuronal circuits that regulate fast-induced food intake and glucoprivic feeding are functionally separable at the circuit level.[11,51] Tools for selective in vivo manipulation of functionally distinct astrocyte subsets that would facilitate a similar type of experimental circuit dissection are not yet available.

The absence of overt morphological or immunoreactivity differences in DVC astrocytes following in vivo glucoprivation may suggest that DVC astrocytes provide metabolic and/or functional support to counter-regulatory neural circuits that is indispensable to their function. Of the currently available tools, future work measuring the regional, state-dependent Ca^{2+} dynamics of DVC astrocytes in vivo during glucose fluctuations may help reconcile our findings with those from ex vivo brain slice imaging.

AUTHOR CONTRIBUTIONS

Alastair J MacDonald: Conceptualization; data curation; formal analysis; funding acquisition; investigation; writing – original draft; writing – review and editing. **Katherine R Pye:** Investigation; writing – review and editing. **Craig Beall:** Conceptualization; funding acquisition; supervision; writing – review and editing. **Kate LJ Ellacott:** Conceptualization; data curation; funding acquisition; supervision; writing – original draft; writing – review and editing.

ACKNOWLEDGEMENTS

The authors would like to thank Matt Isherwood and the staff at the Biological Service Unit at the University of Exeter and Adam Thompson at the RILD building for facilitating this research. The authors would like to thank Ana Miguel Cruz and Paul Weightman Potter for discussions relating to the project. This work was supported by a project grant from Diabetes UK (19/0006035 to Kate L. J. Ellacott and Craig Beall, which funded Alastair J. MacDonald and Katherine R. Pye).

CONFLICT OF INTEREST STATEMENT

The authors have no conflicts of interest to declare.

DATA AVAILABILITY STATEMENT

The data that support the findings of this study are available from the corresponding author upon reasonable request.

ORCID

Kate L. J. Ellacott https://orcid.org/0000-0001-5261-7465

REFERENCES

1. Finley JCW, Katz DM. The central organization of carotid body afferent projections to the brainstem of the rat. *Brain Res*. 1992;572:108-116. doi:10.1016/0006-8993(92)90458-L
2. Grill HJ, Hayes MR. Hindbrain neurons as an essential hub in the neuroanatomically distributed control of energy balance. *Cell Metab*. 2012;16:296-309. doi:10.1016/j.cmet.2012.06.015
3. MacDonald AJ, Ellacott KLJ. Astrocytes in the nucleus of the solitary tract: contributions to neural circuits controlling physiology. *Physiol Behav*. 2020;223(112):982. doi:10.1016/j.physbeh.2020.112982
4. Machado BH. Neurotransmission of the cardiovascular reflexes in the nucleus tractus solitarii of awake rats. *Ann N Y Acad Sci*. 2001;940:179-196. doi:10.1111/j.1749-6632.2001.tb03676.x
5. Ritter S, Dinh TT, Li AJ. Hindbrain catecholamine neurons control multiple glucoregulatory responses. *Physiol Behav*. 2006;89:490-500. doi:10.1016/j.physbeh.2006.05.036
6. Balfour RH, Trapp S. Ionic currents underlying the response of rat dorsal vagal neurones to hypoglycaemia and chemical anoxia. *J Physiol*. 2007;579:691-702. doi:10.1113/jphysiol.2006.126094
7. Balfour RH, Hansen AMK, Trapp S. Neuronal responses to transient hypoglycaemia in the dorsal vagal complex of the rat brainstem. *J Physiol*. 2006;570:469-484. doi:10.1113/jphysiol.2005.098822
8. Boychuk CR, Gyarmati P, Xu H, Smith BN. Glucose sensing by GABAergic neurons in the mouse nucleus tractus solitarii. *J Neurophysiol*. 2015;114:999-1007. doi:10.1152/jn.00310.2015
9. Ritter S, Dinh TT, Zhang Y. Localization of hindbrain glucoreceptive sites controlling food intake and blood glucose. *Brain Res*. 2000;856:37-47. doi:10.1016/S0006-8993(99)02327-6
10. Ritter S, Taylor JS. Vagal sensory neurons are required for lipoprivic but not glucoprivic feeding in rats. *Am J Physiol Regul Integr Comp Physiol*. 1990;258:R1395-R1401. doi:10.1152/ajpregu.1990.258.6.r1395
11. Ritter S, Bugarith K, Dinh TT. Immunotoxic destruction of distinct catecholamine subgroups produces selective impairment of glucoregulatory responses and neuronal activation. *J Comp Neurol*. 2001;432:197-216. doi:10.1002/cne.1097
12. Aklan I, Sayar Atasoy N, Yavuz Y, et al. NTS catecholamine neurons mediate hypoglycemic hunger via medial hypothalamic feeding pathways. *Cell Metab*. 2020;31:313-326.e5. doi:10.1016/j.cmet.2019.11.016
13. Boychuk CR, Smith KC, Peterson LE, et al. A hindbrain inhibitory microcircuit mediates vagally-coordinated glucose regulation. *Sci Rep*. 2019;9:1-12. doi:10.1038/s41598-019-39,490-x
14. Lamy CM, Sanno H, Labouèbe G, et al. Hypoglycemia-activated GLUT2 neurons of the nucleus tractus solitarius stimulate vagal activity and glucagon secretion. *Cell Metab*. 2014;19:527-538. doi:10.1016/j.cmet.2014.02.003
15. Rogers RC, Hermann GE. Hindbrain astrocytes and glucose counterregulation. *Physiol Behav*. 2019;204:140-150. doi:10.1016/j.physbeh.2019.02.025
16. McDougal DH, Viard E, Hermann GE, Rogers RC. Astrocytes in the hindbrain detect glucoprivation and regulate gastric motility. *Auton Neurosci*. 2013;175:61-69. doi:10.1016/j.autneu.2012.12.006
17. McDougal DH, Hermann GE, Rogers RC. Astrocytes in the nucleus of the solitary tract are activated by low glucose or glucoprivation: evidence for glial involvement in glucose homeostasis. *Front Neurosci*. 2013;7:1-10. doi:10.3389/fnins.2013.00249
18. Rogers RC, McDougal DH, Ritter S, Qualls-Creekmore E, Hermann GE. Response of catecholaminergic neurons in the mouse hindbrain to glucoprivic stimuli is astrocyte dependent. *Am J Physiol Regul Integr Comp Physiol*. 2018;315:R153-R164. doi:10.1152/ajpregu.00368.2017
19. Rogers RC, Ritter S, Hermann GE. Hindbrain cytoglucopenia-induced increases in systemic blood glucose levels by 2-deoxyglucose depend on intact astrocytes and adenosine release. *Am J Physiol Regul Integr Comp Physiol*. 2016;310:R1102-R1108. doi:10.1152/ajpregu.00493.2015
20. Marty N, Dallaporta M, Foretz M, et al. Regulation of glucagon secretion by glucose transporter type 2 (glut2) and astrocyte dependent glucose sensors. *J Clin Investig*. 2005;153:3545-3553. doi:10.1172/JCI26309
21. Rogers RC, Burke SJ, Collier JJ, Ritter S, Hermann GE. Evidence that hindbrain astrocytes in the rat detect low glucose with a glucose transporter 2-phospholipase C-calcium release mechanism. *Am J Physiol Regul Integr Comp Physiol*. 2020;318:R38-R48. doi:10.1152/AJPREGU.00133.2019
22. Franklin KBJ, Paxinos G. The Mouse Brain in Stereotaxic Coordinates. 3rd ed. Elsevier/Academic Press; 2008.
23. Cerritelli S, Hirschberg S, Hill R, Balthasar N, Pickering AE. Activation of brainstem proopiomelanocortin neurons produces opioidergic analgesia, bradycardia and bradypnoea. *PLoS One*. 2016;11:1-26. doi:10.1371/journal.pone.0153187
24. MacDonald AJ, Holmes FE, Beall C, Pickering AE, Ellacott KLJ. Regulation of food intake by astrocytes in the brainstem dorsal vagal complex. *GLIA*. 2020;68:1241-1254. doi:10.1002/glia.23774
25. Lewis SR, Ahmed S, Khaimova E, et al. Genetic variance contributes to ingestive processes: a survey of 2-deoxy-D-glucose-induced feeding in eleven inbred mouse strains. *Physiol Behav*. 2006;87:595-601. doi:10.1016/j.physbeh.2005.12.002
26. Schindelin J, Arganda-Carreras I, Frise E, et al. Fiji: an open-source platform for biological-image analysis. *Nat Methods*. 2012;9:676-682. doi:10.1038/nmeth.2019
27. Ferriera TA, Blackman AV, Oyrer J, et al. Neuronal morphometry directly from bitmap images. *Nat Methods*. 2014;11:981-984. doi:10.1038/nmeth.3102
28. Escartin C, Galea E, Lakatos A, et al. Reactive astrocyte nomenclature, definitions, and future directions. *Nat Neurosci*. 2021;24:312-325. doi:10.1038/s41593-020-00783-4
29. Ritter S, Llewellyn-Smith I, Dinh TT. Subgroups of hindbrain catecholamine neurons are selectively activated by 2-deoxy-D-glucose induced metabolic challenge. *Brain Res*. 1998;805:41-54. doi:10.1016/S0006-8993(98)00655-6
30. Armbruster BN, Li X, Pausch MH, Herlitze S, Roth BL. Evolving the lock to fit the key to create a family of G protein-coupled receptors potently activated by an inert ligand. *Proc Natl Acad Sci U S A*. 2007;104:5163-5168. doi:10.1073/pnas.0700293104
31. Lee Y, Messing A, Su M, Brenner M. GFAP promoter elements required for region-specific and astrocyte-specific expression. *GLIA*. 2008;56:481-493. doi:10.1002/glia.20622
32. Adamsky A, Kol A, Kreisel T, et al. Astrocytic activation generates De novo neuronal potentiation and memory enhancement. *Cell*. 2018;174:59-71.e14. doi:10.1016/j.cell.2018.05.002
33. Bonder DE, McCarthy KD. Astrocytic Gq-GPCR-linked IP3R-dependent Ca2+ signaling does not mediate neurovascular coupling in mouse visual cortex in vivo. *J Neurosci*. 2014;34:13139-13150. doi:10.1523/JNEUROSCI.2591-14.2014
34. Bull C, Freitas KCC, Zou S, et al. Rat nucleus accumbens core astrocytes modulate reward and the motivation to self-administer ethanol after abstinence. *Neuropsychopharmacology*. 2014;39:2835-2845. doi:10.1038/npp.2014.135
35. Durkee CA, Covelo A, Lines J, Kofuji P, Aguilar J, Araque A. G i/o protein-coupled receptors inhibit neurons but activate astrocytes and

stimulate gliotransmission. *GLIA*. 2019;67:1076-1093. doi:10.1002/glia.23589
36. Martin-Fernandez M, Jamison S, Robin LM, et al. Synapse-specific astrocyte gating of amygdala-related behavior. *Nat Neurosci*. 2017;20:1540-1548. doi:10.1038/nn.4649
37. Scofield MD, Boger HA, Smith RJ, Li H, Haydon PG, Kalivas PW. Gq-DREADD selectively initiates glial glutamate release and inhibits cue-induced cocaine seeking. *Biol Psychiatry*. 2015;78:441-451. doi:10.1016/j.biopsych.2015.02.016
38. Shigetomi E, Bushong EA, Haustein MD, et al. Imaging calcium microdomains within entire astrocyte territories and endfeet with GCaMPs expressed using adeno-associated viruses. *J Gen Physiol*. 2013;141:633-647. doi:10.1085/jgp.201210949
39. Srinivasan R, Lu TY, Chai H, et al. New transgenic mouse Lines for selectively targeting astrocytes and studying calcium signals in astrocyte processes In situ and In vivo. *Neuron*. 2016;92:1181-1195. doi:10.1016/j.neuron.2016.11.030
40. NamKoong C, Song WJ, Kim CY, et al. Chemogenetic manipulation of parasympathetic neurons (DMV) regulates feeding behavior and energy metabolism. *Neurosci Lett*. 2019;712:134356. doi:10.1016/j.neulet.2019.134356
41. Shi X, Chacko S, Li F, et al. Acute activation of GLP-1-expressing neurons promotes glucose homeostasis and insulin sensitivity. *Mol Metab*. 2017;6:1350-1359. doi:10.1016/j.molmet.2017.08.009
42. Roman CW, Derkach VA, Palmiter RD. Genetically and functionally defined NTS to PBN brain circuits mediating anorexia. *Nat Commun*. 2016;7:1-11. doi:10.1038/ncomms11905
43. Reiner DJ, Mietlicki-Baase EG, McGrath LE, et al. Astrocytes regulate GLP-1 receptor-mediated effects on energy balance. *J Neurosci*. 2016;36:3531-3540. doi:10.1523/JNEUROSCI.3579-15.2016
44. Stein LM, Lhamo R, Cao A, et al. Dorsal vagal complex and hypothalamic glia differentially respond to leptin and energy balance dysregulation. *Transl Psychiatry*. 2020;10:90. doi:10.1038/s41398-020-0767-0
45. Nuzzaci D, Cansell C, Liénard F, et al. Postprandial hyperglycemia stimulates Neuroglial plasticity in hypothalamic POMC neurons after a balanced meal. *Cell Rep*. 2020;30:3067-3078.e5. doi:10.1016/j.celrep.2020.02.029
46. Varela L, Stutz B, Song JE, et al. Hunger-promoting AgRP neurons trigger an astrocyte-mediated feed-forward autoactivation loop in mice. *J Clin Investig*. 2021;131:e144239. doi:10.1172/JCI144239
47. Reeves AMB, Shigetomi E, Khakh BS. Bulk loading of calcium indicator dyes to study astrocyte physiology: key limitations and improvements using morphological maps. *J Neurosci*. 2011;31:9353-9358. doi:10.1523/JNEUROSCI.0127-11.2011
48. Alhadeff AL. Monitoring in vivo neural activity to understand gut-brain signaling. *Endocrinol*. 2021;162:1-12. doi:10.1210/endocr/bqab029
49. Corkrum M, Covelo A, Lines J, et al. Dopamine-evoked synaptic regulation in the nucleus Accumbens requires astrocyte activity. *Neuron*. 2020;105:1036-1047.e5. doi:10.1016/j.neuron.2019.12.026
50. Tan HE, Sisti AC, Jin H, et al. The gut–brain axis mediates sugar preference. *Nature*. 2020;580:511-516. doi:10.1038/s41586-020-2199-7
51. Hudson B, Ritter S. Hindbrain catecholamine neurons mediate consummatory responses to glucoprivation. *Physiol Behav*. 2004;82:241-250. doi:10.1016/j.physbeh.2004.03.032
52. Batiuk MY, Martirosyan A, Wahis J, et al. Identification of region-specific astrocyte subtypes at single cell resolution. *Nat Commun*. 2020;11:1-15. doi:10.1038/s41467-019-14198-8
53. Mastitskaya S, Turovsky E, Marina N, et al. Astrocytes modulate baroreflex sensitivity at the level of the nucleus of the solitary tract. *J Neurosci*. 2020;40:3052-3062. doi:10.1523/JNEUROSCI.1438-19.2020
54. McDougal DH, Hermann GE, Rogers RC. Vagal afferent stimulation activates astrocytes in the nucleus of the solitary tract via AMPA receptors: evidence of an atypical neural-glial interaction in the brainstem. *J Neurosci*. 2011;31:14037-14045. doi:10.1523/JNEUROSCI.2855-11.2011
55. Marina N, Turovsky E, Christie IN, et al. Brain metabolic sensing and metabolic signaling at the level of an astrocyte. *GLIA*. 2018;66:1185-1199. doi:10.1002/glia.23283
56. Vance KM, Rogers RC, Hermann GE. PAR1-activated astrocytes in the nucleus of the solitary tract stimulate adjacent neurons via NMDA receptors. *J Neurosci*. 2015;35:776-785. doi:10.1523/JNEUROSCI.3105-14.2015
57. Cheng W, Gordian D, Ludwig MQ, Pers TH, Seeley RJ, Myers MG. Hindbrain circuits in the control of eating behaviour and energy balance. *Nat Metab*. 2022;4:826-835. doi:10.1038/s42255-022-00606-9
58. Perez C, Sclafani A. Cholecystokinin conditions flavor preferences in rats. *Am J Physiol Regul Integr Comp Physiol*. 1991;260:R179-R185.
59. Lawrence CB, Ellacott KLJ, Luckman SM. PRL-releasing peptide reduces food intake and may mediate satiety signaling. *Endocrinology*. 2002;143:360-367. doi:10.1210/endo.143.2.8609
60. Lachey JL, D'Alessio DA, Rinaman L, Elmquist JK, Drucker DJ, Seeley RJ. The role of central glucagon-like peptide-1 in mediating the effects of visceral illness: differential effects in rats and mice. *Endocrinology*. 2005;146:458-462. doi:10.1210/en.2004-0419
61. Thiele TE, Van Dijk G, Campfield LA, et al. Central infusion of GLP-1, but not leptin, produces conditioned taste aversions in rats. *Am J Physiol Regul Integr Comp Physiol*. 1997;272:R726-R730. doi:10.1152/ajpregu.1997.272.2.r726
62. Clyburn C, Carson KE, Smith CR, Travagli RA, Browning KN. Brainstem astrocytes control homeostatic regulation of caloric intake. *J Physiol*. 2023;4:801-829. doi:10.1113/jp283566
63. Chen J, Cheng M, Wang L, et al. A vagal-NTS neural pathway that stimulates feeding. *Curr Biol*. 2020;30:986-3998.e5. doi:10.1016/j.cub.2020.07.084
64. Ludwig MQ, Cheng W, Gordian D, et al. A genetic map of the mouse dorsal vagal complex and its role in obesity. *Nat Metab*. 2021;3:530-545. doi:10.1038/s42255-021-00363-1
65. Alhadeff AL, Holland RA, Zheng H, Rinaman L, Grill HJ, De Jonghe BC. Excitatory hindbrain-forebrain communication is required for cisplatin-induced anorexia and weight loss. *J Neurosci*. 2017;37:362-370. doi:10.1523/JNEUROSCI.2714-16.2016

SUPPORTING INFORMATION

Additional supporting information can be found online in the Supporting Information section at the end of this article.

How to cite this article: MacDonald AJ, Pye KR, Beall C, Ellacott KLJ. Impact of chemogenetic activation of dorsal vagal complex astrocytes in mice on adaptive glucoregulatory responses. *J Neuroendocrinol*. 2023;35(8):e13315. doi:10.1111/jne.13315